ACS APPLIED MATERIALS & INTERFACES

Research Article

www.acsami.org

Fabrication of Biodegradable Polymeric Nanofibers with Covalently Attached NO Donors

Kathryn A. Wold,[†] Vinod B. Damodaran,[‡] Lucas A. Suazo,[§] Richard A. Bowen,[∥] and Melissa M. Reynolds*[,†,‡]

[†]School of Biomedical Engineering, Colorado State University, 204 Engineering Building, Fort Collins, Colorado 80523, United States

[‡]Department of Chemistry, Colorado State University, 1872 Campus Delivery, Fort Collins, Colorado 80523, United States

[§]Department of Mechanical Engineering, Colorado State University, Fort Collins, Colorado 80523, United States

[∥]Department of Biomedical Sciences, Colorado State University, 1680 Campus Delivery, Fort Collins, Colorado 80523, United States

Supporting Information

ABSTRACT: Many common wound healing aids are created from biodegradable polymeric materials. Often, these materials are unable to induce complete healing in wounds because of their failure to prevent infection and promote cell growth. This study reports the development of therapeutic materials aimed at overcoming these limitations through the release of a naturally occurring antimicrobial agent from a porous, polymeric fiber scaffold. The antimicrobial character was achieved through the release of nitric oxide (NO) while the porous structure was fabricated through electrospinning polymers into nanofibers. Three variations of the polymer poly(lactic-*co*-glycolic-*co*-hydroxymethyl propionic acid) (PLGH) modified to include thiol and NO groups were investigated. Fibers of the modified polymers exhibited smooth, bead free morphologies with diameters averaging between 200 and 410 nm. These fibers were deposited in a random manner to create a highly porous fibrous scaffold. The fibers were found to release NO under physiological pH and temperature and have the capacity to release 0.026 to 0.280 mmol NO g^{-1}. The materials maintained their fibrous morphological structure after this exposure to aqueous conditions. The sustained morphological stability of the fiber structure coupled to their extended NO release gives these materials great potential for use in wound healing materials.

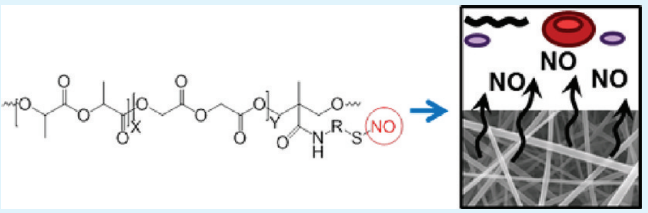

KEYWORDS: *electrospinning, nanofiber, biodegradable, nitric oxide, therapeutic release, antibacterial, wound healing*

INTRODUCTION

Wounds caused by traumatic injury or disease often require medical interventions for proper healing to occur since the natural biochemical processes, required to restore function, are disrupted.[1] As such, artificial materials exhibiting therapeutic action are often applied to chronic wounds in an attempt to facilitate healing.[2] However, current materials often fail to prevent infection and promote cell growth, which leads to further complications.[3,4] An ideal material for wound care would (1) prevent infection at the wound site and (2) support cell growth by mimicking the natural extracellular matrix (ECM) on which cells move and grow.

Today's advanced wound care materials are designed to contain antimicrobial agents to prevent bacterial adhesion at the wound site in order to avoid infection. Common agents incorporated into wound care devices include antibiotics or other antimicrobial agents such as the antibiotic cefazolin[5] or silver.[6] More recently, materials have been tailored with cell lytic enzymes to target specific bacteria.[7] However, antibiotic resistant bacterial strains are becoming more common and the effectiveness of any one antibiotic toward treating multiple strains of bacteria remains a serious health concern.

Previous research has demonstrated that materials capable of releasing predictable levels of nitric oxide (NO), a naturally occurring biological molecule, could be capable of preventing and treating several infection causing pathogens.[8−10] Compared to other common antimicrobial agents, NO is appealing since it functions to prevent bacterial adhesion through a variety of mechanisms. Nitric oxide induces membrane damage and DNA deamination in bacterial cells while remaining noncytotoxic to normal human skin cells. Because of these varied mechanisms of action, wound treatments employing NO may be less likely to develop bacterial resistance. In addition, unlike many antibiotics, NO has proven effective at killing multiple disease-causing bacterial strains, making it a broad spectrum antimicrobial agent.[9,11,12]

Not only does NO provide protection from infection, it also plays a significant role in numerous biological functions, including modulating hemostasis, reducing inflammation,[13] and promoting the healing of the skin.[14] As such, several groups

Received: March 1, 2012
Accepted: June 4, 2012
Published: June 4, 2012

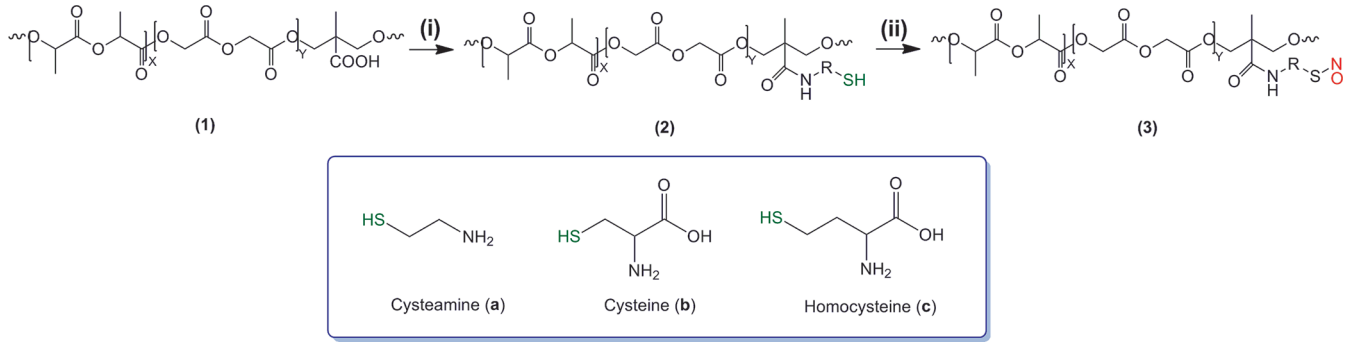

Figure 1. Scheme illustrating the sysnthesis of *S*-nitrosated PLGH derivatives (i) NHS, EDC, NH_2-R-SH and (ii) *t*-butyl nitrite, DCM:CH_3OH (1:2).

have reported the development of NO releasing polymers for medical applications.[15−20] The incorporation of NO into wound healing materials is also beneficial as NO helps to promote collagen deposition, a key factor in natural wound repair. As the wound healing process occurs over a period of days, prolonged release of NO is desirable for promoting antimicrobial effects as the initial biological activities aimed to rid the wound of bacteria take place during the first two days of the normal wound healing process,[21,22] and potentially longer in the case of chronic wound situations. Toward this end, storing NO in a polymeric scaffold could provide the ideal route for safe storage and ideal delivery of NO in medical applications.

The structure of the polymeric material used to deliver NO is crucial to the functioning of the device, and must therefore be tailored with the goal of promoting cell growth and proliferation, as well as releasing therapeutic amounts of NO. Electrospun nanofibers have been extensively studied as versatile biomedical device materials, including those involved in wound healing. This is due to their increased surface area, tunable mechanical properties, and ability to mimic the ECM.[23,24] In particular, these properties serve to increase proliferation and movement of cells from the outer edges to the center of the wound. Although not used clinically, several natural and synthetic polymer formulations have been developed into nanofibers and investigated as materials to aid in the repair and healing of skin.[25−27] These studies demonstrate the promise biodegradable electrospun polymer materials have in supporting cell growth and accelerating the wound healing process. Others have shown that electrospun blends of poly-L-lactide (PLLA) and poly(D,L)-lactide-*co*-glycolide (PLGA) allow complete cell migration into the scaffold material during wound healing[25] and electrospun fibers consisting of a blends of PLGA and collagen accelerate early stage wound healing.[27]

The incorporation of NO release capability into a biodegradable nanofibrous scaffold would provide a 2-fold healing potential and have significant advantages over current material platforms. Tailored NO release would provide a natural therapeutic toward adverse bacterial responses whereas the fibrous matrix would mimic the natural ECM and serve to support cell attachment. Previous works on NO releasing fibers developed from polymers blended with NO donors have been reported. Coneski et al. developed microfibers by blending PROLI/NO with polymer solutions of Tecoflex polyurethane and poly(vinyl chloride).[28] Lopez-Jaramillo et al. developed a multilayer NO releasing transdermal patch where NO (generated from acidified nitrite with ascorbic acid) was encapsulated in Tecophilic polymer nanofibers.[29] In both of these cases, the fibers created were biostable. Others have reported the development of degradable NO releasing nanofibers.[30,31] While NO release has been demonstrated from these materials, the NO release rates are rapid or not well characterized. However, by using blended NO donors, chances of donor leaching are a serious concern toward the biomedical application of these materials. Consequently a stable incorporation of the NO donor as well as its specificity and controlled release capability are ideal requirements. As such, it would be beneficial to have a stable and prolonged NO release to provide a long-term therapeutic effect.

Herein, we examine an electrospinning process developed to prepare NO releasing nanofibers with prolonged NO release from variations of thiol-derivatized poly(lactic-*co*-glycolic-*co*-hydroxymethyl propionic acid) (PLGH) functionalized to incorporate NO onto the polymer backbone. The morphology of the fibers, NO release characteristics, and effects of short-term aqueous exposure to the morphology of the fibers were evaluated. Finally, preliminary studies investigating the antibacterial efficacy resulting from these materials will be presented. Taken together, this work describes the development of a series of novel electrospun NO releasing materials that have both the requisite morphologies and controllable NO release properties that could be ultimately used to promote wound healing.

EXPERIMENTAL SECTION

Materials. *N*,*N*′-dimethylformamide (DMF) and phosphate buffered saline (PBS) were purchased from EMD chemicals (Gibbstown, NJ, U.S.A.), and tertahydrofuran (THF) was purchased from Mallinckrodt chemicals (Phillipsburg, NJ, U.S.A.). *N*-hydroxysuccinimide (NHS) and *t*-butyl nitrite were purchased from Acros Organics (Morris Plains, NJ, U.S.A.). All other chemicals were procured from Sigma-Aldrich (St. Louis, MO, U.S.A.) and used as received.

Methods. *Polymer Synthesis.* Thiolated and *S*-nitrosated PLGH derivatives were prepared in house following our early reported procedure[32] illustrated in Figure 1. In brief, a carboxyl functionalized polymer backbone (PLGH) was prepared by a ring-opening melt polymerization of L-lactide (LA, 85% w/w) and glycolide (GL, 10% w/w) with 2,2′-bis(hydroxymethyl propionic acid) (HMPA, 5% w/w) using stannous octoate as the catalyst. The pendant carboxyl groups were modified to thiol terminals (**2**) by covalently conjugating a number of aminothiol derivatives such as cysteamine, cysteine and homocysteine through amide linkages using 1-ethyl-3-(3-dimethylaminopropyl) carbodiimide hydrochloride (EDC.HCl) and *N*-hydroxysuccinimide (NHS) in anhydrous DMF. The pendent thiol terminals were nitrosated with *t*-butyl nitrite (pretreated with 10% w/v EDTA disodium salt) using a mixture of dichloromethane:methanol (1:2) to yield the corresponding *S*-nitrosated polymer derivatives (**3**). The *S*-nitrosation was performed in an EPA-certified amber vial, free of

metal ion contaminants that could result in premature *S*-nitrosothiol decomposition. The structural and morphological properties of all the intermediate and finished products were extensively characterized using ^{1}H NMR, FTIR-ATR, GPC, DSC, TGA, and SAXS, and reported previously.[32] Thiol content of the thiolated derivatives was calculated by integrating proton intensities from the ^{1}H NMR spectrum of the respective thiol derivatives as reported previously.[32]

Electrospinning. PLGH, its thiolated derivatives, and the *S*-nitrosated derivatives were dissolved in a 75:25 w/w mixture of THF and DMF to obtain 10 to 40 w/w% solutions. Each polymer solution was drawn into nanofibers by a modified electrospinning process reported previously.[5] A 1 mL syringe with a 22 G blunt tip needle was loaded with polymer solution and inserted into a variable speed syringe pump (Kent Scientific Corp., Torrington, CT, U.S.A.) with a flow rate of 0.2 mL h^{-1}. Various potentials were applied via a high-voltage power supply (Gamma High Voltage Research, Ormond Beach, FL, U.S.A.). Fibers were collected on glass slides attached to a grounded copper plate. The temperature of the electrospinning environment was 25 °C, and the humidity was 15%. As light can induce decomposition of *S*-nitrosothiols, the nitrosated polymers were electrospun with the syringe guarded from light exposure and the lights off in the room.

Viscosity Measurements. Viscosity of polymer solutions at concentrations used during electrospinning were recorded using a stress-controlled AR-G2 rheometer (TA Instruments, New Castle, DE, U.S.A.) equipped with at 40 mm, 2° steel cone. Sample sizes of approximately 600 μL of 10% PLGH-cysteamine, 20% PLGH-cysteine, 40% PLGH-homocysteine, and 20% of each *S*-nitrosated PLGH-cysteamine, -cysteine, and —homocysteine were used, and viscosities for each material were measured in triplicate. Measurements were recorded in Pa s at 25 °C under sheer rates ranging from 10 to 100 s^{-1}.

Conductivity Measurements. Conductivity of polymer solutions was measured using an accumet XL50 dual channel pH/ion/conductivity meter (Fisher Scientific). The conductivity probe was placed in a glass vial containing 1 mL polymer solution, and measurements were recorded in μS/cm^{-1}.

Fiber Morphological Stability under Physiological Conditions. *S*-nitrosated polymer fibers spun onto glass slides were submersed in 10 mL PBS in separate glass vials. Vials were covered with a rubber septum and nitrogen was bubbled into the system. Temperature was maintained at 37 °C. After a period of 48 h, samples were removed and rinsed with deionized (DI) water.

Fiber Analysis. Scanning electron microscopy (JEOL JSM-6500F, JEOL U.S.A., Peabody, MA, U.S.A.) was used to visualize fiber morphology. Images were acquired using an accelerating voltage of 15 kV. Before analysis, samples were sputter coated with 10 nm gold. The average diameter of the polymer fibers were measured from the original SEM micrographs at 10 000× magnification using Adobe Photoshop CS5 software as described previously from Duan et al.[33] The diameter of 25 fibers from three different SEM micrograph frames was recorded, for a total of 75 measured fibers for each polymer system. The number of measurements recorded was 75 based on previously published work.[28]

Nitric Oxide Release. Real-time NO release from polymer fibers was determined using a Siever's chemiluminescence NO analyzer (NOA 280i, GE Analytical, Boulder, CO, USA) using methods published previously.[17] Briefly, the instrument was calibrated before each analysis using nitrogen as the zero gas and a standard 45 ppm NO gas. Approximately 5 mg of *S*-nitrosated electrospun polymer samples were accurately weighed and inserted into an NOA measurement cell, containing 30 mL deoxygenated 10 mM phosphate buffered saline (PBS, pH 7.4) submersed in a water bath to maintain system temperature at 37 °C and shielded from direct exposure to light using aluminum foil. Measurements were recorded in triplicate at a data interval of 5 s at a gas sampling rate of 200 mL min^{-1} with a cell pressure of 9.7 Torr and an oxygen pressure of 6 psig. Since the released NO is constantly removed from the sample cell to be detected via chemiluminescence, the NO release profiles show the real-time NO released at each time point. As a result, the real-time curves shown have not been curve fit.

In Vitro Antibacterial Studies. Thirty milligrams of *S*-nitrosated PLGH-cysteamine was dissolved in 1.8 mL PBS buffer, shaken, and heated to 37 °C for two minutes. A 0.2 mL aliquot of solution containing the bacteria, *Acinetobacter baumannii*, was added to each vial. The vials were then shaken and heated at 37 °C for 2 h. A 0.1 mL sample from each of the three vials was taken and diluted by a factor of 10, five times. These samples were then spread on BHI culture plates and left to incubate for 48 h. The number of colonies on each of the plates was then recorded.

Statistical Analysis. All experiments were performed in triplicate. Data is expressed as a mean ± standard deviation. Statistical analysis was performed using the *t* test and significance was considered at $p \leq 0.05$.

RESULTS AND DISCUSSION

Nanofiber Formation and Morphology. In this study, an electrospinning method was developed to create a porous scaffold structure with preserved NO release function from degradable *S*-nitrosothiol PLGH polymers. Previous groups have studied the use of unmodified PLGA nanofibers or blends of unmodified PLGA with other polymers for applications in biomedical devices, especially those related to wound healing.[5,27] We began with the parameters reported by Katti et al.[5] and varied the voltage applied, polymer flow rate through the syringe, and polymer concentration until uniform nanofibers were achieved.[34,35] For this work, applied voltages between 8 and 15 kV and polymer concentrations between 10 and 40% in a 75:25 w/w solution of THF/DMF were investigated. Distance between the nozzle and collecting plate were maintained at a constant 15 cm. By examining the SEM micrographs, we found uniform, bead free fibers were successfully spun from thiolated and nitrosated PLGH derivatives using the parameters summarized in Table 1. Specifically, an applied voltage of

Table 1. Summary of Optimized Electrospinning Conditions

parameter variables	optimized conditions
polymer concentration	10−40%
applied voltage	10 kV
flow rate	0.2 mL h^{-1}
solvent system	THF/DMF (75:25 w/w)
distance between the nozzle and collector	15 cm
electrospinning time	30 min

10 kV and a flow rate of 0.2 mL h^{-1} produced uniform fiber morphologies for all polymers evaluated: unmodified PLGH, thiolated PLGH, and nitrostaed PLGH. However, different concentrations of the polymers were necessary to produce bead free fibers across all polymer derivatives.

In general, polymer concentrations between 10 and 40 w/w % were necessary to produce fibers from the thiolated polymers, whereas fibers prepared from the nitrosated polymers were able to be electrospun at a constant polymer concentration (20 w/w %). For both PLGH-cysteamine and PLGH-homocysteine, the use of a 20 w/w% solution resulted in severe bead formation. By altering polymer concentrations, bead free fibers of PLGH-cysteamine and PLGH-homocysteine were successfully created using 10 w/w% and 40 w/w% solutions, respectively.

Representative SEM micrographs of the nanofibers from all of the polymer derivatives are shown in Figure 2. Both the thiolated and nitrosated electrospun polymers resulted in highly porous structures with interconnected pores distributed throughout the fibrous structure. All fibers exhibited a random

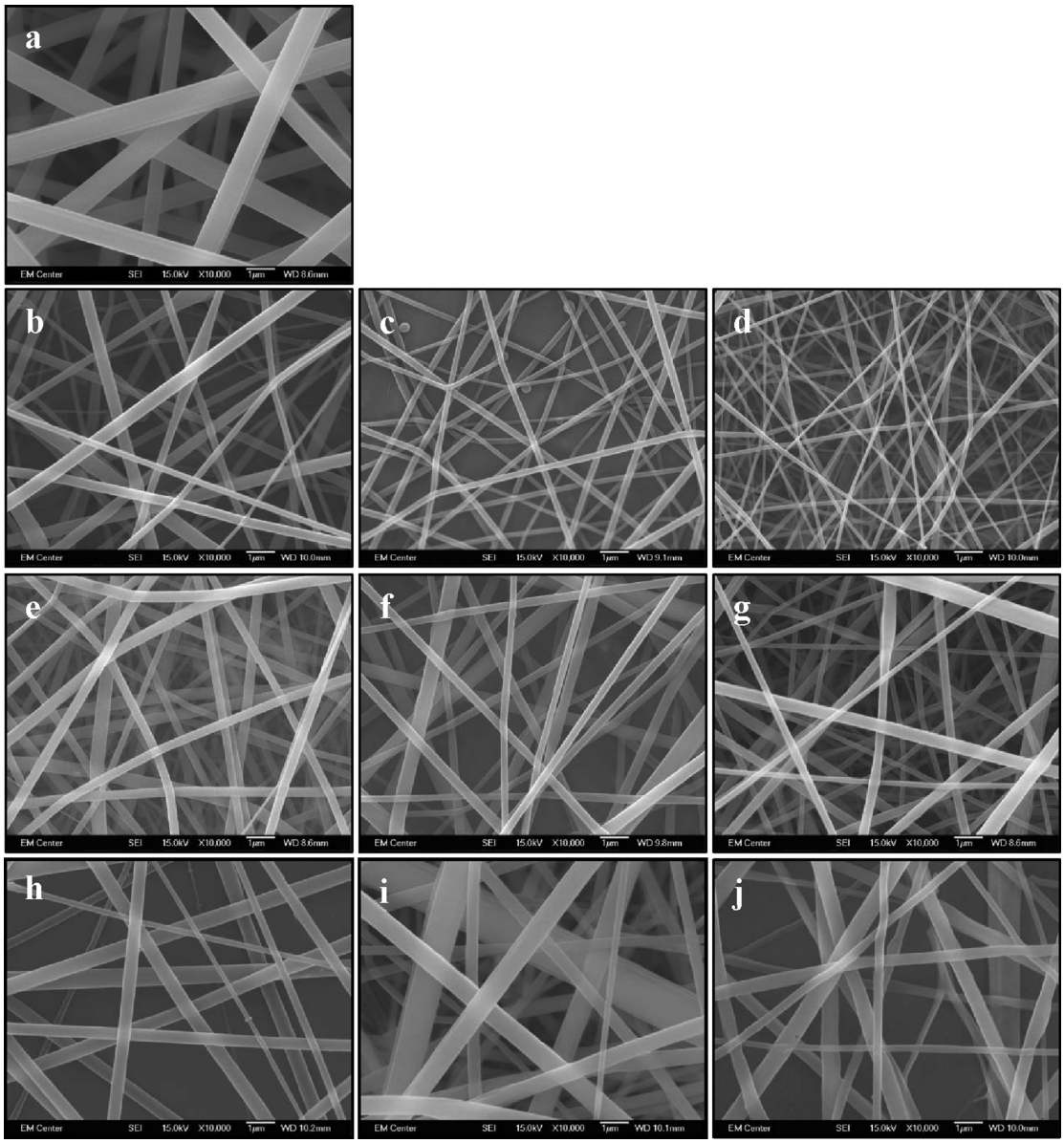

Figure 2. SEM images at 10 000× of electrospun nanofibers of (a) PLGH, (b) PLGH-cysteamine, (c) PLGH-cysteine, (d) PLGH-homocysteine, (e) *S*-nitrosated PLGH-cysteamine, (f) *S*-nitrosated PLGH-cysteine, and (g) *S*-nitrosated PLGH-homocysteine. Electrospun fibers after exposure to physiological pH and temperature in PBS for 48 h: (h) *S*-nitrosated PLGH-cysteamine, (i) *S*-nitrosated PLGH-cysteine, and (j) *S*-nitrosated PLGH-homocysteine.

orientation. The overall shape, orientation, and pore size of the fibers are similar regardless of the identity of the thiol (i.e., cysteine, cysteamine, and homocysteine) or the subsequent nitrosation. Further, the scaffolds were similar to that of unmodified PLGH. The fiber morphology exhibits high surface-to-volume area and high porosity in a three-dimensional structure. This is important as the nanofiber structure mimics that of the natural ECM thereby capable of supporting cellular attachment.[36]

The fiber diameter obtained for the unmodified PLGH polymer (803 ± 205 nm) was found to be comparable to that reported for other electrospun fibers prepared with PLGA of similar composition (760 ± 210 nm).[34,37] The fiber diameters of this unmodified PLGH materials were found to be almost twice to four times larger than the fibers electrospun from the thiolated and *S*-nitrosated polymer analogs (Table 2). Fiber diameters ranged from an average of 200−330 nm for the thiolated PLGH polymers and 250 to 410 nm for the *S*-nitrosated polymers. However, no trend in fiber diameter was observed for the thiolated or *S*-nitrosated materials regardless of the specific thiol system used. The mean values for the thiolated and *S*-nitrosated polymers are similar (roughly between 200 and 400 nm) and are within one standard deviation of each other. Although the standard deviations are large for all samples,

Table 2. Average Fiber Diameters for Electrospun PLGH Polymers[a]

polymer	fiber diameter (nm)
PLGH	803 ± 205
PLGH-cysteamine	330 ± 78
PLGH-cysteine	200 ± 205
PLGH-homocysteine	216 ± 116
PLGH-cysteamine SNO	250 ± 93
PLGH-cysteine SNO	410 ± 145
PLGH-homocysteine SNO	281 ± 116

[a] $n = 75$.

subsequent analysis of the measured diameters from each SEM image (n = 75) did not reveal a trend with regards to (a) the diameter size, (b) the location on the image, or (c) whether each of the polymer samples had fiber diameters with significant outliers (see histograms in Supporting Information). Taken together, the images as well as the measured fiber diameters suggest that the resulting diameters are randomly dispersed but fall within relative ranges of each other. The fiber diameters within the natural ECM are also random and range from several tens to hundreds of nanometers.[38] This makes these nanofibers an ideal representation of the natural ECM environment.

Although polymer concentration seemingly had the most significant influence on the ability to form nanofibers, fiber morphology is also known to be influenced by solution viscosity and conductivity. To determine the contribution of viscosity and conductivity on the ability to form NO releasing nanofibers, additional experiments were performed. Viscosity measurements were performed for all thiolated and nitrosated PLGH polymers at the concentrations which successfully produced the electrospun fibers. All polymer derivatives exhibited Newtonian viscosity across sheer stresses ranging from 10 to 100 s^{-1}. As a result, final viscosity measurements were determined by averaging the values over this sheer range. As shown in Table 3,

Table 3. Viscosities of PLGH Polymer Solutions

	viscosity (Pa·s)	
polymer	thiol	SNO
PLGH-cysteamine	0.00201 ± 8.27 × 10^{-5}	0.00319 ± 0.00038
PLGH-cysteine	0.00762 ± 0.00045	0.00886 ± 0.00092
PLGH-homocysteine	0.03637 ± 0.00491	0.00795 ± 0.00056

the differences in viscosity were significant for the thiol-modified PLGH polymers, with the 10% PLGH-cysteamine solution exhibiting the lowest viscosity (0.0020 Pa s) and the 40% PLGH-homocysteine solution exhibiting the highest viscosity (0.0364 Pa s). The nitrosated polymers (all in solutions of 20% w/w%) were also all statistically different from each other. The measured viscosities ranged from 0.0032 Pa s for *S*-nitrosated PLGH-cysteamine solution to 0.0080 Pa s for *S*-nitrosated PLGH-homocysteine solution. The solution containing the PLGH-cysteine derivative was the only solution where the same polymer concentration was used to produce electrospun fibers from both thiolated and *S*-nitrosated materials. On the other hand, the viscosity of the polymer solutions were altered by the nitrosation process as the thiolated and *S*-nitrosated polymers exhibit statistically different viscosities. Taken together, these results show no apparent relationship between polymer concentrations and viscosity under fiber-forming concentrations of the polymers. Even the *S*-nitrosated polymers, which were all electrospun at the same concentration, exhibit different viscosities.

Another factor known to influence fiber formation is solution conductivity. It has been reported that more uniform fibers with fewer bead defects can be produced by increasing the solution conductivity;[39] however, there is conflicting literature as to the role conductivity plays in fiber diameter.[40,41] To explore this further, we measured the conductivity of the thiolated (10 wt %) and nitrosated (20 wt %) PLGH-cysteamine polymer solutions that produced bead free fibers. We found that functionalization with a nitroso group significantly decreased the solution conductivity. The reason for this observed changed in solution conductivity may be due to the decrease in SH moieties.

On the basis of these experiments, we have determined neither viscosity nor conductivity provide adequate explanations for the variations in thiolated polymer concentrations necessary for forming nanofibers. The effect of polymer concentration on nanofiber formation however may be best explained by analyzing the thiol content of each polymer derivative. All of the polymer solutions had the same amount of thiols present (i.e., ∼0.7 mmol·g^{-1}), where, as reported previously,[32] each of the thiol modified PLGH polymers had different loadings of the respective thiol groups cysteamine (0.57 ± 0.03 mmol·g^{-1}), cysteine (0.39 ± 0.02 mmol·g^{-1}), or homocysteine (0.18 ± 0.05 mmol·g^{-1}). When each polymer solution was normalized for thiol content (mmol·g^{-1}) in the electrospinning solution, the thiol content in solution was found to be similar across polymer derivatives (See Table 4).

Table 4. Thiol Content of Polymers Normalized for Concentration in Electrospinning Solution

	electrospinning process	
polymer	polymer concentration in solution (% w/w)	net thiol content in polymer solution (mmol g^{-1})
PLGH-cysteamine	10	0.06
PLGH-cysteine	20	0.08
PLGH-homocysteine	40	0.07

This correlation between thiol content and solution concentration suggests that the extent of thiols in solution may have the greatest influence on fiber formation for these materials. This observed behavior may arise from the extensive cross-linking of the polymer chains through disulfide linkages under the given applied voltage. Consequently, to prevent this disulfide bond formation, a lower polymer concentration for higher thiol content polymers was required to produce bead free nanofibers. This explanation is also consistent with the observation that all of the nitrosated polymers (cysteamine, homocysteine, and cysteine PLGH derivatives) were successfully electrospun at a solution concentration of 20 wt %. After nitrosation, far fewer thiol groups exist, thus eliminating the possibility of disulfide bond formation. As an example, PLGH-homocysteine has 96% of thiols converted to *S*-nitrosothiols after the nitrosation process while PLGH-cysteamine has a 93% conversion. In contrast, PLGH-cysteamine demonstrates only a 43% conversion.[32]

As no correlations were found to exist between solution conductivity, viscosity, and nanofiber formation, we hypothesize that the difference in diameter size can be explained by considering the lattice structures of the unmodified and modified polymers. Incorporation of the thiol functionalities onto the polymer backbone increases the randomness in the polymer lattice. This, in turn, increases the self-repulsion interactions between the polymer chains. Consequently, these repulsive forces enhance the stretching force of the polymer jet under the applied field[42] and result in comparably smaller fiber diameters for the thiolated and *S*-nitrosated PLGH derivatives compared to unmodified PLGH.

NO Release. The ability of the electrospun fibers to maintain their NO release capabilities after fabrication is important if the resulting material is to be practically useful for the treatment of bacterial infections. Thus, our primary aim was to demonstrate that nanofibers could be formed from *S*-nitrosated PLGH derivatives without diminishing their capability of releasing NO. We also wanted to investigate the effect of the different thiols on NO release profiles of the

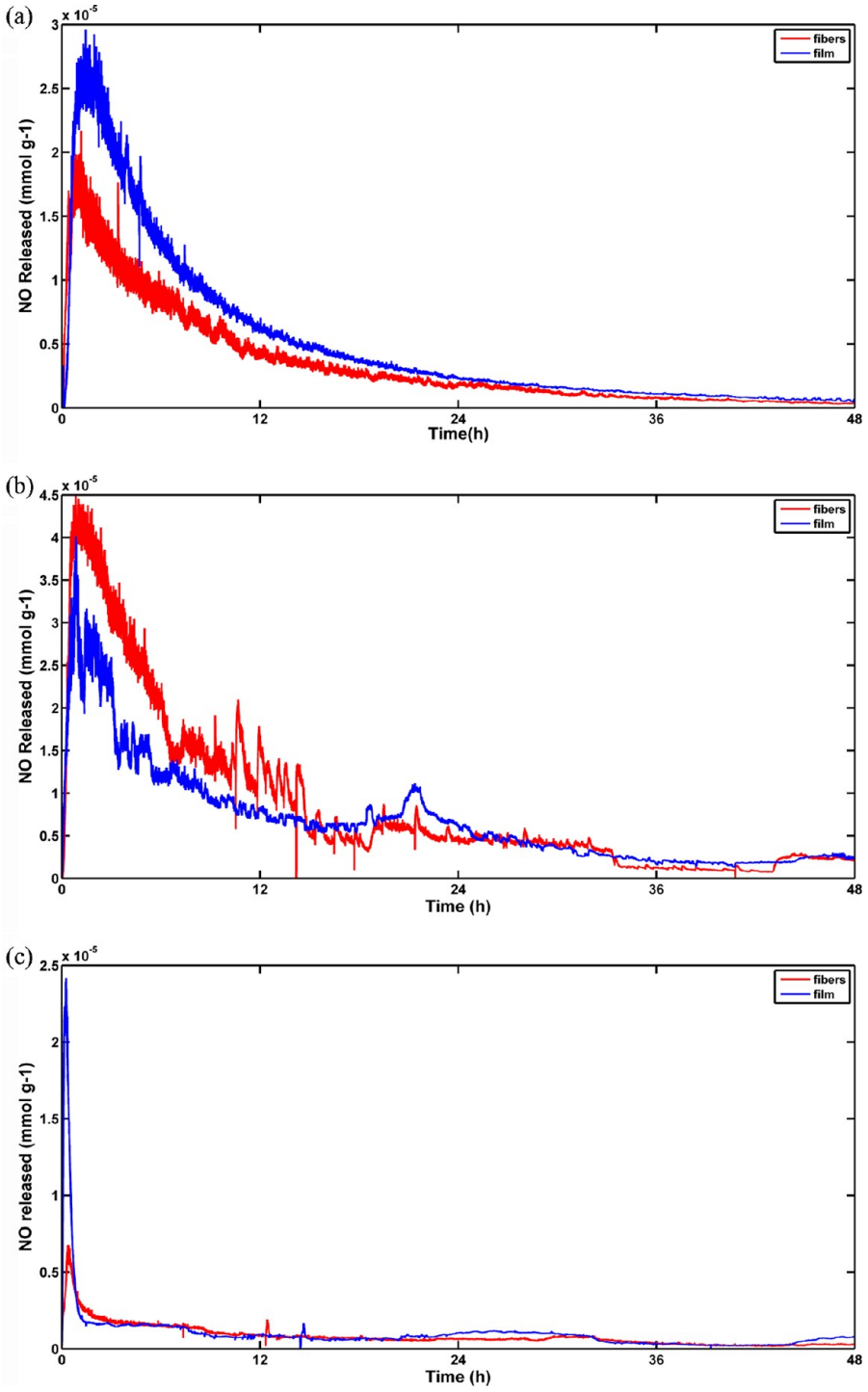

Figure 3. Representative NO release kinetic profiles from individual thin film and electrospun *S*-nitrosated polymers under experimental physiological conditions (10 mM PBS buffer/pH 7.4/37 °C) for 48 h: (a) *S*-nitrosated PLGH-cysteine, (b) *S*-nitrosated PLGH-cysteamine, and (c) *S*-nitrosated PLGH-homocysteine.

resulting polymers. In this regard, we evaluated the extent of NO release from nanofibers under physiological pH and temperature in PBS buffer using a highly specific, real-time chemiluminescence NO analyzer. Above, NO release results from the nanofibers are presented in terms of (1) comparison to thin-films and (2) comparison to the various thiol analogs.

Comparison between Thin Films and Nanofibers. Figure 3 shows the representative real-time NO release profiles normalized for the weight of each polymer analog as a function of fabrication method: electrospun nanofibers and spin-coated films. The shapes of the curves and relative magnitude of release demonstrate that the high voltages applied to the polymer solution during the electrospinning process do not alter the NO storage capabilities or release kinetics of the material compared with other processing methods. While the total amount of NO released from the electrospun *S*-nitrosated PLGH-homocysteine (0.033 ± 0.007 mmol·g^{-1}) was found to be statistically similar to the spin-coated films (0.026 ± 0.004 mmol·g^{-1}), the electrospun *S*-nitrosated PLGH-cysteine and -cysteamine materials exhibited statistically significant

differences ($p \leq 0.05$) in the total moles of NO released after 48 h (see Table 5). For these materials, however, no trend in the loss of NO release capability was observed. Thin film *S*-nitrosated PLGH-cysteine exhibited an NO release of 0.155 ± 0.009 mmol·g^{-1}, which was greater than the amount of NO released from the electrospun material (0.110 ± 0.007 mmol g^{-1}). In contrast, the electrospun *S*-nitrosated PLGH-cysteamine demonstrated a greater NO release over 48 h when compared to the same polymer processed as a thin film (0.281 ± 0.016 mmol g^{-1} as compared to 0.241 ± 0.004 mmol g^{-1}). These small differences in NO release after processing can be attributed to the relative stability of the *S*-nitrosothiol materials and not the fabrication process itself.

Table 5. Comparison between NO Released over 48 h from Polymers Processed into Thin Films and Nanofibers

	NO released after 48 h[b]	
S-nitrosated polymer	thin film[a] (mmol g^{-1})	nanofibers (mmol g^{-1})
PLGH-cysteamine SNO	0.241 ± 0.004	0.281 ± 0.016
PLGH-cysteine SNO	0.155 ± 0.009	0.110 ± 0.007
PLGH-homocysteine SNO	0.033 ± 0.007	0.026 ± 0.004

[a]As reported previously.[32] [b]Under physiological conditions (10 mM PBS/pH 7.4/37 °C).

Comparison between *S*-Nitrosated Nanofibers. The NO release profiles of all *S*-nitrosated nanofibers can be characterized by an initial rapid release of NO followed by a slower release rate over the remaining 48 h (see Figure 4).

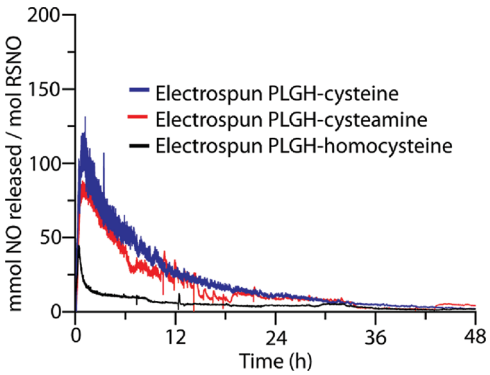

Figure 4. Comparison of NO release from electrospun polymers over 48 h.

In general, the higher storage capacity materials exhibited the larger initial rate of NO release. Nanofibers made from *S*-nitrosated PLGH-cysteamine demonstrated the greatest release rate over 48 h, followed by the cysteine and homocysteine analogs. The instantaneous NO release peaked between 30 min to 1 h for all three polymer systems. The relatively lower NO release level of the homocysteine derivative can be attributed to the relative higher stability of the *S*-nitrosated homocysteine species compared to the cysteine and cysteamine derivatives under the release conditions. The trends in NO release from the different *S*-nitrosated nanofibers are consistent with those of the thin films.

While we report the amount of NO released from the nanofibers over 48 h, none of these materials had exhausted their NO release capacity during this time period. The 48 h release profiles for S-nitrosated PLGH-cysteamine and *S*-nitrosated PLGH-cysteine fit well to an exponential function. Based on this fit, the *S*-nitrosated cysteamine and cysteine nanofibers would be expected to release NO for 85 h before reaching baseline. On the other hand, the NO release from the homocysteine analog quickly achieved a steady state release level that was maintained for 46 h after the initial 2 h spike. As such, if these fibers maintained this rate of NO release, the material would actively release NO for 198 h before reaching baseline.

One of the major advantages of this system is the sustained release of NO over multiple days. In previous work,[28] NO release from composite electrospun fiber material occurred rapidly over the period of minutes. Our materials provide continuous release of NO over long periods of time, creating a better solution in the prevention of bacterial infection.

Nanofiber Morphological Stability after Immersion in PBS. For a nanofiber material to function to promote wound healing, the fiber morphology of the material must be maintained in physiological conditions long enough to promote cell attachment. Degradation properties of the bulk PLGH materials have been previously conducted and demonstrated a complete degradation of the material over nearly 40 weeks for PLGH-cysteamine, 30 weeks for PLGH-cysteine and 20 weeks for PLGH and PLGH-homocysteine polymer derivatives.[32] As such, we wanted to ensure the fibers were capable of maintaining morphology under physiological conditions in the first 48 h, the time needed to begin suitable cell attachment. The exposure of these fibers to physiological conditions for 48 h demonstrated that the electrospun matrix maintains its characteristic fibrous form. Figure 2 shows the random orientation of the fibers after NO release. The maintenance of fiber form over a period of days is beneficial for applications in wound healing when the material must initially remain intact in order to provide a strong scaffold for cell growth and proliferation. On the basis of the previous findings with the bulk material, it is expected the scaffold will completely degrade over a longer time-scale. The complete degradation of the material is intended and advantageous after cell infiltration into the scaffold has occurred.

Preliminary Antimicrobial Evaluation. In preliminary studies to determine whether the NO released from these materials was sufficient to kill bacteria, we treated *Acinetobacter baumannii* with *S*-nitrosated PLGH-cysteamine for 2 h at 37 °C in PBS buffer. As shown in Figure 5, the NO release profile presented an initial burst of NO release followed by a slower

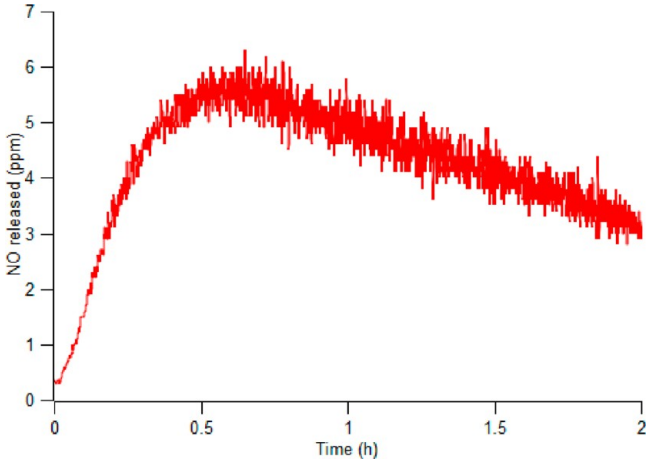

Figure 5. NO release profile of 30 mg *S*-nitrosated PLGH-cysteamine used during bacterial studies.

decay. Integrating the area under the curve, the treatment dosage of 0.0035 mmol of NO resulted in a 96% reduction in the bacterial counts. This kill efficiency is higher than any other reported NO delivery material to date. Previous studies using NO releasing sol–gel derived xerogels in an adhesion model have shown a bacterial reduction by 70 to 80%.[43,44] On the basis of these preliminary studies, the estimated quantities required to achieve nearly 96% bacterial reduction using various polymeric forms are summarized in Table 6. Future studies are underway to understand the dose–response relationship of the NO releasing materials in various fabrication forms.

Table 6. Approximate Amount of Materials Required to Achieve 96% Reduction in the Bacterial Count

	polymeric form	
S-nitrosated polymer	film qty (mg)	nanofiber qty (mg)
PLGH-cysteamine SNO	23.3	19.4
PLGH-cysteine SNO	150.5	175.2

CONCLUSIONS

In this study, a series of thiolated and NO releasing biodegradable PLGH polymers were successfully electrospun to create nanofiber scaffolds capable of continuous NO release over a period of days when submerged in PBS under physiological temperature and pH. Each material exhibited its own unique NO release properties. Short-term exposure to aqueous conditions did not alter the morphology of the fibers as all materials were shown to maintain their nanofibrous forms after 48 h. The development of biodegradable nanofibers containing covalently attached NO donors may provide a novel paradigm for applications in wound healing. The nanofibers act to mimic the natural extracellular matrix while controlled and extended NO release provides bactericidal activity. With both properties combined into one material, further investigation into the impact of these materials in preventing bacterial responses and promoting cell attachment in wounded tissue are warranted.

ASSOCIATED CONTENT

Supporting Information

Histograms of nanofiber diameter dispersions for all electrospun PLGH materials. This material is available free of charge via the Internet at http://pubs.acs.org.

AUTHOR INFORMATION

Corresponding Author

*E-mail: Melissa.Reynolds@colostate.edu. Telephone: (970) 491-3775. Fax: (970) 491-1801.

Notes

The authors declare no competing financial interest.

ACKNOWLEDGMENTS

We would like to thank Dr. Liberatore (Chemical and Biological Engineering, Colorado School of Mines) for use of the viscometer and Nathan Crawford (Chemical and Biological Engineering, Colorado School of Mines) for assistance in obtaining the viscosity data. KW and VD were supported by the Department of Defense Congressional Directed Medical Research Program. LS is a Boettcher scholar and MR is a Boettcher investigator. We would like to further acknowledge Colorado State University (Fort Collins, CO) for funding this work.

REFERENCES

(1) Singer, A. J.; Clark, R. A. F. *N. Engl. J. Med.* **1999**, *341*, 738.
(2) van der Veen, V. C.; Boekema, B. K. H. L.; Ulrich, M. M. W.; Middelkoop, E. *Wound Repair Regener.* **2011**, *19*, s59.
(3) Macri, L.; Clark, R. A. F. *Skin Pharmacol. Physiol.* **2009**, *22*, 83.
(4) Mi, F. L.; Wu, Y. B.; Shyu, S. S.; Schoung, J. Y.; Huang, Y. B.; Tsai, Y. H.; Hao, J. Y. *J. Biomed. Mater. Res.* **2002**, *59*, 438.
(5) Katti, D. S.; Robinson, K. W.; Ko, F. K.; Laurencin, C. T. *J. Biomed. Mater. Res., Part B* **2004**, *70B*, 286.
(6) Hospenthal, D. R.; Murray, C. K.; Andersen, R. C.; Blice, J. P.; Calhoun, J. H.; Cancio, L. C.; Chung, K. K.; Conger, N. G.; Crouch, H. K.; D'Avignon, L. C.; Dunne, J. R.; Ficke, J. R.; Hale, R. G.; Hayes, D. K.; Hirsch, E. F.; Hsu, J. R.; Jenkins, D. H.; Keeling, J. J.; Martin, R. R.; Moores, L. E.; Petersen, K.; Saffle, J. R.; Solomkin, J. S.; Tasker, S. A.; Valadka, A. B.; Wiesen, A. R.; Wortmann, G. W.; Holcomb, J. B. *J. Trauma Acute Care Surg.* **2008**, 64.
(7) Miao, J. J.; Pangule, R. C.; Paskaleva, E. E.; Hwang, E. E.; Kane, R. S.; Linhardt, R. J.; Dordick, J. S. *Biomaterials* **2011**, *32*, 9557.
(8) Seabra, A. B.; Martins, D.; Simoes, M.; da Silva, R.; Brocchi, M.; de Oliveira, M. G. *Artif. Organs* **2010**, *34*, E204.
(9) Martinez, L. R.; Han, G.; Chacko, M.; Mihu, M. R.; Jacobson, M.; Gialanella, P.; Friedman, A. J.; Nosanchuk, J. D.; Friedman, J. M. *J. Invest. Dermatol.* **2009**, *129*, 2463.
(10) Hetrick, E. M.; Schoenfisch, M. H. *Chem. Soc. Rev.* **2006**, *35*, 780.
(11) Mihu, M. R.; Sandkovsky, U.; Han, G.; Friedman, J. M.; Nosanchuk, J. D.; Martinez, L. R. *Virulence* **2010**, *1*, 62.
(12) Deupree, S. M.; Schoenfisch, M. H. *Acta Biomater.* **2009**, *5*, 1405.
(13) Frost, M. C.; Reynolds, M. M.; Meyerhoff, M. E. *Biomaterials* **2005**, *26*, 1685.
(14) Witte, M. B.; Barbul, A. *American J. Surg.* **2002**, *183*, 406.
(15) Mowery, K. A.; Schoenfisch, M. H.; Saavedra, J. E.; Keefer, L. K.; Meyerhoff, M. E. *Biomaterials* **2000**, *21*, 9.
(16) Damodaran, V. B.; Reynolds, M. M. *J. Mater. Chem.* **2011**, *21*, 5870.
(17) Reynolds, M. M.; Hrabie, J. A.; Oh, B. K.; Politis, J. K.; Citro, M. L.; Keefer, L. K.; Meyerhoff, M. E. *Biomacromolecules* **2006**, *7*, 987.
(18) Zhao, H. C.; Serrano, M. C.; Popowich, D. A.; Kibbe, M. R.; Ameer, G. A. *J. Biomed. Mater. Res., Part A* **2010**, *93A*, 356.
(19) Bohls-Masters, K.; Leibovich, S.; Belem, P.; West, J.; Poole-Warren, L. *Wound Repair Regener.* **2002**, *10*, 286.
(20) Masters, K. S. B.; Lipke, E. A.; Rice, E. E. H.; Liel, M. S.; Myler, H. A.; Zygourakis, C.; Tulis, D. A.; West, J. L. *J. Biomater. Sci., Polym. Ed.* **2005**, *16*, 659.
(21) Oberyszyn, T. M. *Front. Biosci.* **2007**, *12*, 2993.
(22) Eming, S. A.; Krieg, T.; Davidson, J. M. *J. Invest. Dermatol.* **2007**, *127*, 514.
(23) Hunley, M. T.; Long, T. E. *Polym. Int.* **2008**, *57*, 385.
(24) Kumbar, S. G.; et al. *Biomed. Mater.* **2008**, *3*, 034002.
(25) Blackwood, K. A.; McKean, R.; Canton, I.; Freeman, C. O.; Franklin, K. L.; Cole, D.; Brook, I.; Farthing, P.; Rimmer, S.; Haycock, J. W.; Ryan, A. J.; MacNeil, S. *Biomaterials* **2008**, *29*, 3091.
(26) Powell, H. M.; Supp, D. M.; Boyce, S. T. *Biomaterials* **2008**, *29*, 834.
(27) Liu, S. J.; Kau, Y. C.; Chou, C. Y.; Chen, J. K.; Wu, R. C.; Yeh, W. L. *J. Membr. Sci.* **2010**, *355*, 53.
(28) Coneski, P. N.; Nash, J. A.; Schoenfisch, M. H. *ACS Appl. Mater. Interfaces* **2011**, *3*, 426.
(29) Lopez-Jaramillo, P.; Rincon, M. Y.; Garcia, R. G.; Silva, S. Y.; Smith, E.; Kampeerapappun, P.; Garcia, C.; Smith, D. J.; Lopez, M.; Velez, I. D. *Am. J. Trop. Med. Hyg.* **2010**, *83*, 97.
(30) Liu, H. A.; Balkus, K. J. *Chem. Mater.* **2009**, *21*, 5032.
(31) Bohlender, C.; Wolfram, M.; Goerls, H.; Imhof, W.; Menzel, R.; Baumgaertel, A.; Schubert, U. S.; Mueller, U.; Frigge, M.; Schnabelrauch, M.; Wyrwa, R.; Schiller, A. *J. Mater. Chem.* **2012**, *22*, 8785.
(32) Damodaran, V. B.; Joslin, J. M.; Wold, K. A.; Lantvit, S. M.; Reynolds, M. M. *J. Mater. Chem.* **2012**, *22*, 5990.

(33) Duan, B.; Wu, L. L.; Yuan, X. Y.; Hu, Z.; Li, X. L.; Zhang, Y.; Yao, K. D.; Wang, M. *J. Biomed. Mater. Res., Part A* **2007**, *83A*, 868.
(34) You, Y.; Min, B.-M.; Lee, S. J.; Lee, T. S.; Park, W. H. *J. Appl. Polym. Sci.* **2005**, *95*, 193.
(35) Bashur, C. A.; Dahlgren, L. A.; Goldstein, A. S. *Biomaterials* **2006**, *27*, 5681.
(36) Sill, T. J.; von Recum, H. A. *Biomaterials* **2008**, *29*, 1989.
(37) Xin, X.; Hussain, M.; Mao, J. J. *Biomaterials* **2007**, *28*, 316.
(38) Ma, Z. W.; Kotaki, M.; Inai, R.; Ramakrishna, S. *Tissue Eng.* **2005**, *11*, 101.
(39) Pham, Q. P.; Sharma, U.; Mikos, A. G. *Tissue Eng.* **2006**, *12*, 1197.
(40) Mit-uppatham, C.; Nithitanakul, M.; Supaphol, P. *Macromol. Chem. Phys.* **2004**, *205*, 2327.
(41) Jiang, H. L.; Fang, D. F.; Hsiao, B. S.; Chu, B.; Chen, W. L. *Biomacromolecules* **2004**, *5*, 326.
(42) Meng, Z. X.; Zheng, W.; Li, L.; Zheng, Y. F. *Mater. Chem. Phys.* **2011**, *125*, 606.
(43) Nablo, B. J.; Chen, T. Y.; Schoenfisch, M. H. *J. Am. Chem. Soc.* **2001**, *123*, 9712.
(44) Nablo, B. J.; Rothrock, A. R.; Schoenfisch, M. H. *Biomaterials* **2005**, *26*, 917.